

Direct measurement of the energy thresholds to conformational isomerization. II. 3-indole-propionic acid and its water-containing complex

Jasper R. Clarkson, Esteban Baquero, and Timothy S. Zwier^{a)}

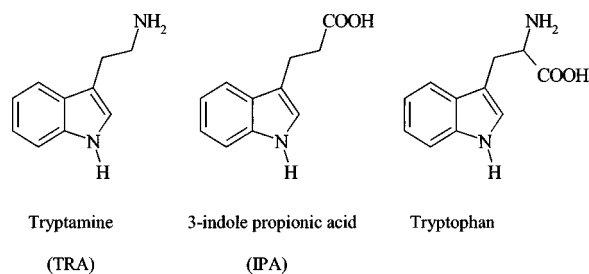
Department of Chemistry, 560 Oval Drive, Purdue University, West Lafayette, Indiana 47907-2084

(Received 7 March 2005; accepted 1 April 2005; published online 7 June 2005)

The methods of stimulated emission pumping-hole-filling spectroscopy (SEP-HFS) and population transfer spectroscopy (SEP-PTS) were used to place direct experimental bounds on the energetic barriers to conformational isomerization in 3-indole-propionic acid (IPA) and its water-containing complex. By contrast with tryptamine (Paper I), IPA has only two conformations with significant population in them. The structures of the two conformers are known from previous work [P. M. Felker, *J. Phys. Chem.* **96**, 7844 (1992)]. The energy thresholds for $A \rightarrow B$ and $B \rightarrow A$ isomerizations are placed at 854 and 754 cm^{-1} , respectively. Lower bounds on the isomerization barrier in the two directions are determined from the last transition *not* observed in the SEP-PT spectra. These are placed at 800 and 644 cm^{-1} for $A \rightarrow B$ and $B \rightarrow A$, respectively. The combined results place bounds on the relative energies of the A and B minima, with $E(B) - E(A) = 46 - 210 \text{ cm}^{-1}$. Like the IPA monomer, the IPA- H_2O complex forms two conformational isomers. Both these isomers incorporate the water molecule as a bridge between the carbonyl and OH groups of the carboxylic acid. Previous rotational coherence measurements (L. L. Connell, Ph.D. thesis, UCLA, 1991) have determined that these complexes retain the same IPA conformational structure as the monomers. SEP-PTS and SEP-HFS were carried out on the IPA- H_2O complexes. It was demonstrated that it is possible to use SEP to drive conformational isomerization between the two conformational isomers of IPA- H_2O . Bounds on the energy barriers to conformational isomerization are not effected greatly by the presence of the water molecule, with $E_{\text{barrier}}(A \rightarrow B) = 771 - 830 \text{ cm}^{-1}$ and $E_{\text{barrier}}(B \rightarrow A) = 583 - 750 \text{ cm}^{-1}$. This is a simple consequence of the fact that the barrier is an intramolecular barrier, and the water molecule is held fixed in the COOH pocket, where it interacts with the ring only peripherally during the isomerization process. Finally, changes in the SEP-PT spectral intensity in transitions near the top of the barrier to isomerization as a function of the position of SEP excitation relative to the pulsed valve exit provide some insight to the competition between vibrational relaxation and isomerization in a molecule the size of IPA. © 2005 American Institute of Physics. [DOI: 10.1063/1.1924455]

I. INTRODUCTION

In the preceding paper (Paper I),¹ the methods of stimulated emission pumping-hole-filling spectroscopy (SEP-HFS) and stimulated emission pumping-population transfer spectroscopy² (SEP-PTS) were employed to place bounds on the energy barriers to isomerization in tryptamine (TRA). In that case, there were seven conformational isomers with significant population. This tested the method's ability to selectively study the barriers to conformational isomerization for specific $X \rightarrow Y$ conformational reactant-product pairs, even in a complicated situation where many conformations were present simultaneously in the expansion. In the present paper, we extend these measurements to three-indole-propionic acid (IPA). IPA and TRA differ from tryptophan by the removal of a NH_2 or COOH group, respectively.



In many ways, IPA is far easier to study with hole-filling methods than TRA, because IPA has only two conformational isomers with significant population in the supersonic expansion. Figure 1(a) shows these two conformations, determined from rotational coherence measurements of Felker.³ Our primary interest then is to use IPA as a second test case for obtaining accurate barrier heights (for $A \rightarrow B$ and $B \rightarrow A$) and relative energies of the minima [$E_{\text{min}}(B) - E_{\text{min}}(A)$], for comparison with *ab initio* and density-functional theory (DFT).

Second, the high signal-to-noise ratio of the scans in IPA enables us to explore the dependence of the population transfer spectra on the collisional cooling conditions in the expansion.

^{a)}Authors to whom correspondence should be addressed. Electronic mail: zwier@purdue.edu

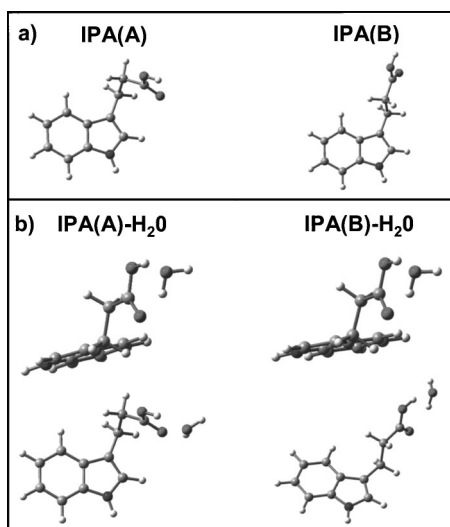


FIG. 1. Assigned structures of the experimentally observed conformational minima of (a) IPA and (b) IPA-H₂O complexes. The assignments are consistent with previous work. The side view of the IPA-H₂O complexes highlight the insertion of the water molecule into the -COOH pocket resulting in a H-bonded bridge between the C=O and the -OH sites.

sion. Because the experimental protocol requires recoiling the laser-excited conformations prior to probing the product downstream in the expansion, conformational isomerization necessarily occurs in competition with vibrational relaxation into the initially excited well. As we shall see, for vibrational energies near the top of the barrier, faster collisional cooling reduces the isomerization product yield. These data will be used to explore the potential of the method for extracting energy-dependent isomerization rates.

Finally, the method of SEP-population transfer spectroscopy is applied here for the first time to a molecular complex, IPA-H₂O. In principle, such measurements are a powerful new probe of the influence of solvent molecules bound at particular sites on the barriers to a flexible molecule's conformational isomerization. In the case of IPA, the COOH group provides a pocket in which water binds preferentially, forming a doubly H-bonded bridge between the C=O and OH groups, as shown in Fig. 1(b).⁴ The IPA-H₂O complex exists in the same two IPA conformations as the monomer,⁵ suggesting that this single water molecule has little influence on the inherent conformational energetics of the IPA minima. Here the SEP-population transfer spectra are used to study the influence of the water molecule on the barrier to isomerization. As we shall see, in IPA-H₂O, the energy barriers so determined are very similar to those in the monomer, consistent with the fact that the water molecule is held in a position remote from the conformational reaction coordinate (internal rotation about the C(α)-C(β) bond).

II. METHODS

A. Experiment

The experimental setup has been described in detail (Paper I).¹ Briefly, solid samples of IPA were resistively heated to 400–410 K and entrained in a flow of helium at a backing pressure of 6 bars. A pulsed valve (1.2-mm orifice) operating

at 20 Hz is used to cool the molecules into their conformational zero-point levels (ZPL) in a supersonic expansion. Total flow rates of 2×10^{-3} bar L/s in a 1.0–1.5-ms gas pulse were used. Water clusters were formed by flowing helium through a pickup cell at room temperature and adjusting the flow until a 0.1% water concentration was achieved. The experimental conditions used to obtain SEP and SEP-population transfer spectra of IPA monomer and the IPA-H₂O complex were similar to those used in the preceding paper on tryptamine.¹ The three UV sources employed were tunable dye lasers pumped by the second harmonic of Nd:YAG (yttrium aluminum garnet) lasers using Fluorescein 27 in both the pump and probe and a R6G/610 mix in the dump.

B. Calculations

Full optimizations of the two lowest-energy minima of IPA and IPA-H₂O were carried out using the GAUSSIAN03 suite of programs⁶ employing the Becke3LYP^{7,8} functional with the 6-31+G(d) (Ref. 9) basis set.¹⁰ Transition state structures were located by using quadratic linear searches employing the QST3 method in G03. The optimized transition state structures were verified by the presence of a single imaginary frequency in the harmonic normal modes.

III. RESULTS

A. LIF spectra

Figure 2 presents the LIF excitation spectrum of IPA monomer and its water complexes in the $S_1 \leftarrow S_0$ origin region. UV-UV hole-burning spectroscopy by Carney *et al.*⁴ confirmed that all observed transitions of IPA monomer can be accounted for by two conformations. The $S_1 \leftarrow S_0$ origin transitions (A at 34 965 cm⁻¹ and B at 34 918 cm⁻¹) have been the subject of rotational coherence studies,³ which have determined that IPA(A) and IPA(B) are the gauche and anti structures shown in Fig. 1(a), respectively.

The $S_1 \leftarrow S_0$ origin transitions of the IPA-H₂O complex are also labeled in the figure. Rotational coherence studies⁵ have shown that the IPA(A) and IPA(B) monomer conformations are retained in the water complexes, as one might surmise based on the close proximity of the origin transitions of the monomer and water complexes. Resonant ion-dip infrared spectra⁴ of IPA(A)-H₂O and IPA(B)-H₂O are consistent with the water molecule forming a H-bonded bridge between the C=O and OH sites of the COOH group.

To observe the population changes induced by the SEP process, the majority of the IPA-H₂O complexes must be formed prior to SEP excitation. Figure 2(b) presents a downstream LIF scan taken at the probe position of $x/D=6$ while Figure 2(c) presents the LIF taken at the SEP excitation position of $x/D=2.5$. Here x is the distance from the nozzle orifice, and D is the orifice diameter (1.2 mm in this case). The transition intensities of the IPA-H₂O complex transitions have reached their final fractional abundance relative to the monomer transitions by 3.0 mm downstream, which is the distance where SEP excitation occurs.

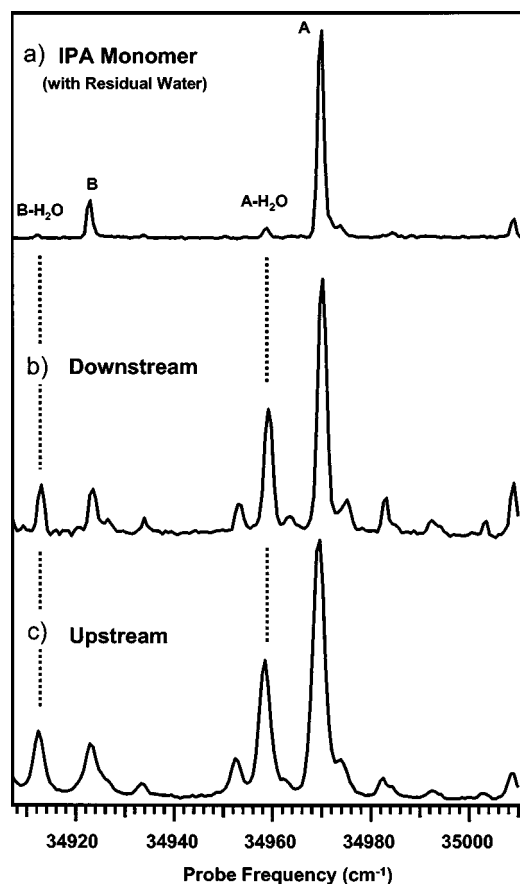


FIG. 2. (a) Laser-induced fluorescence excitation spectrum of IPA and IPA-H₂O complexes in the region of the $S_1 \leftarrow S_0$ origins. (b) The “downstream” LIF spectrum taken at the probe position of $x/D=6$. (c) The “upstream” spectrum taken at the SEP excitation position of $x/D=2.5$. The intensities of the IPA-H₂O transitions have reached their final fractional abundance relative to the monomer by $x/D=2.5$.

B. SEP spectra

Figures 3(a) and 3(c) show SEP spectra of the IPA(A) and IPA(B) monomers, respectively, following selective excitation of their $S_1 \leftarrow S_0$ origin transitions. These spectra were recorded by depleting the fluorescence from the selected origin transition with the tuned dump laser, as described in Paper I. The abscissa is plotted as the energy (in wave numbers) above the vibrational zero-point level of the excited monomer.

The SEP spectra of the two monomer conformations are very similar to one another, with strong transitions localized on the indole ring, and hence rather insensitive to the conformation of the propionic acid side chain. Note the different energy ranges of the two SEP spectra, which highlight the region of interest for the SEP-PT spectra.

The analogous scans of IPA(A)-H₂O and IPA(B)-H₂O are shown in Figs. 4(a) and 4(c), respectively. Once again, the spectra are similar to one another, and to those of IPA monomer, consistent with the remote site of attachment for the water molecule relative to the indole ring.

C. SEP-population transfer spectra

1. IPA monomer

Since the IPA monomer has only two populated conformations in the expansion, there are only two reactant-product

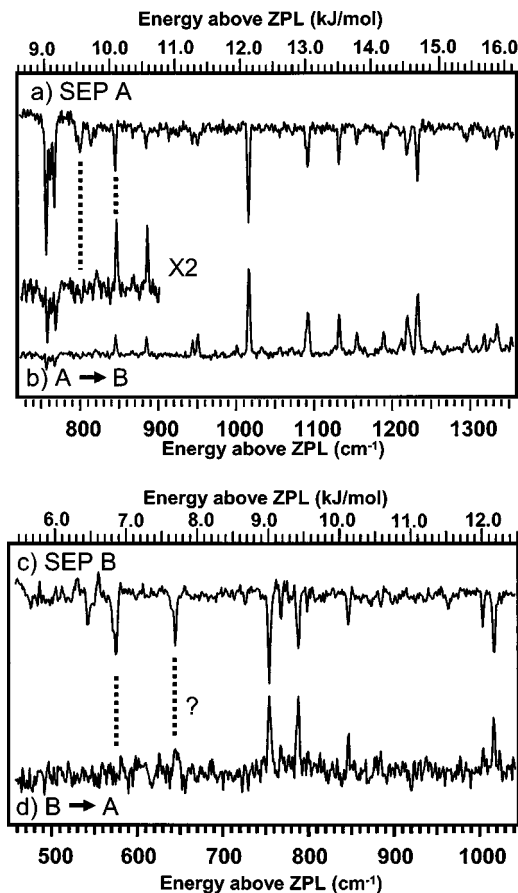


FIG. 3. (a) SEP spectra of IPA-A. (b) SEP-population transfer (PT) spectrum for A-B. The inset is expanded $\times 2$ to highlight the sharp onset (upper bound) for population gain at 854 cm^{-1} . (c) SEP spectrum of IPA-B. (d) SEP-PT spectrum for B-A. The question mark signifies the questionable bound due to poor signal to noise.

pairs of consequence; namely, IPA(A) \rightarrow IPA(B) and IPA(B) \rightarrow IPA(A). SEP-PT spectra of these two processes are shown in Figs. 3(b) and 3(d), respectively. Since excitation of A can transfer population only to B, and vice versa, the population transfer is efficient, creating SEP-PT gains with excellent signal-to-noise ratio, so that even weak transitions in the SEP spectra are observable in the SEP-PT spectra.

For the IPA(A) \rightarrow IPA(B) isomerization, the first observed and last unobserved transitions [marked by dashed lines in Fig. 3(b)] are at 854 and 800 cm^{-1} above the A ZPL, respectively. In this case, the intense transitions in the SEP spectra at 757 and 767 cm^{-1} are just below this region. Their complete absence from the SEP-PT spectrum of A \rightarrow B illustrates the sharp nature of the threshold for the isomerization. The small depletions observed in their place result from a competition between SEP and fluorescence. Below threshold, the dump laser drives population exclusively back down into the A reactant well. The population change monitored in SEP-PT spectroscopy is the difference in population in the product channel with or without the dump laser present. If fluorescence creates a ground-state energy distribution which extends above the barrier to isomerization, then the SEP process will decrease the amount of product B formed, producing a small depletion in below-barrier transitions, as observed.

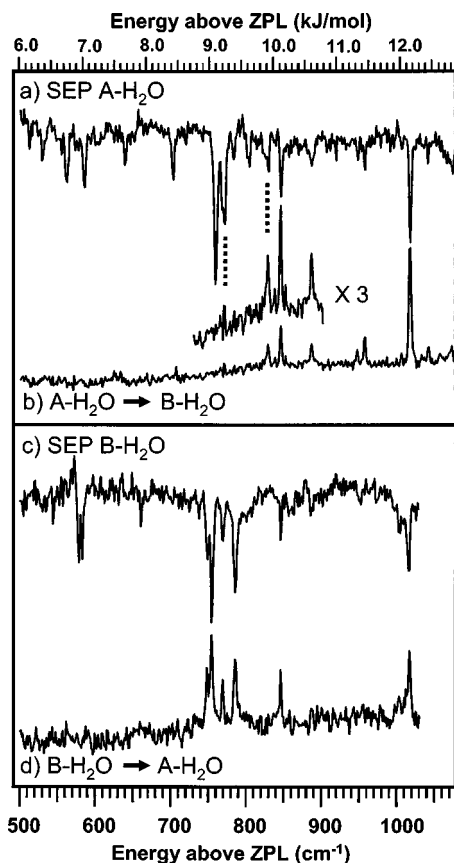


FIG. 4. (a) SEP spectrum of $A\text{-H}_2\text{O}$. (b) SEP-PT spectrum of $A\text{-H}_2\text{O} \rightarrow B\text{-H}_2\text{O}$. The inset is magnified by 3. (c) SEP spectrum of $B\text{-H}_2\text{O}$. (d) SEP-PT spectrum of $B\text{-H}_2\text{O} \rightarrow A\text{-H}_2\text{O}$.

The first transition observed in the $\text{IPA}(B) \rightarrow \text{IPA}(A)$ spectrum of Fig. 3(d) is the intense transition at 754 cm^{-1} . Determination of the last unobserved transition is less obvious in $B \rightarrow A$ spectrum, since there is a small bump at the position of the 644 cm^{-1} transition, just above the level of the noise. A firm lower bound occurs at 575 cm^{-1} , but the intensity of the 644-cm^{-1} transition is just large enough we will use this transition as the lower bound for further discussion. Using the 644-cm^{-1} transition as a lower bound, the combined results place bounds on the relative energies of the A and B minima, with the ZPL of conformer B $46\text{--}210\text{ cm}^{-1}$ above the ZPL of A :

$$\begin{aligned} E(B) - E(A) &= [E_{\text{thresh}}(A \rightarrow B) - E(A)] \\ &\quad - [E_{\text{thresh}}(B \rightarrow A) - E(B)] \\ &= (800 - 854) - (644 - 754) \end{aligned}$$

TABLE I. Calculated and experimental energy thresholds and relative energies of IPA and IPA-H₂O complexes.

Isomerization reaction	Calculated E_{thresh}^c	Experimental E_{thresh}	Calculated $E(B) - E(A)$	Experimental $E(B) - E(A)$
$\text{IPA}(A) \rightarrow (B)^a$	750	800-854	8	46-210
$\text{IPA}(B) \rightarrow (A)^a$	742	644-754
$\text{IPA}(A)\text{-H}_2\text{O} \rightarrow (B)\text{-H}_2\text{O}^b$	780	771-830	8	21-247
$\text{IPA}(B)\text{-H}_2\text{O} \rightarrow (A)\text{-H}_2\text{O}^b$	772	583-750

^aAll energies are reported in wavenumbers (cm^{-1}) relative to $\text{IPA}(A)$, the lowest-energy minimum.

^bAll energies are reported in wavenumbers (cm^{-1}) relative to the $\text{IPA}(A)\text{-(H}_2\text{O)}_1$ lowest-energy minimum.

^cCalculated values are DFT/6-31+G^{*} zero-point corrected $1\text{ kcal/mol} = 4.184\text{ kJ/mol} = 350\text{ cm}^{-1}$.

$$= 46\text{--}210\text{ cm}^{-1}.$$

2. IPA-H₂O

The LIF spectrum showing both the monomer and water complex transitions is shown in Fig. 2(b). The majority of the $\text{IPA-H}_2\text{O}$ complexes must be formed prior to SEP excitation to observe any changes induced by the SEP excitation. The intensities of the $\text{IPA-H}_2\text{O}$ complex transitions have reached their final fractional abundance relative to the monomer transitions by 3.0-mm downstream [Fig 2(c)], which is the distance where SEP excitation occurs. Therefore, cluster formation between the SEP excitation and the probe position is not contributing and any changes in the population can be attributed to the SEP excitation process.

The analogous PT spectra of the $A \rightarrow B$ and $B \rightarrow A$ isomerization processes in the $\text{IPA-H}_2\text{O}$ complex are shown in Figs. 4(b) and 4(d), respectively. The thresholds occur at nearly identical positions to those in the monomer, with first observed/last unobserved transitions occurring at $771/830\text{ cm}^{-1}(A \rightarrow B)$ and $644/754\text{ cm}^{-1}(B \rightarrow A)$. The missing band at 644 cm^{-1} in the $B \rightarrow A$ spectrum is a less firm lower bound than that in $A \rightarrow B$, because the former band's intensity is so weak in the SEP spectrum. Combining the threshold data for the $A \rightarrow B$ and $B \rightarrow A$ directions yields bounds on the relative energies of the minima of

$$\begin{aligned} E[\text{IPA-H}_2\text{O}(B)] - E[\text{IPA-H}_2\text{O}(A)] \\ &= (771 - 830) - (644 - 754) \\ &= 21\text{--}247\text{ cm}^{-1}. \end{aligned} \quad (1)$$

3. Comparison with calculations

Table I compares the experimental measurements of the thresholds and the relative energies of the minima with the computed values for the minima and transition states calculated at the DFT Becke 3LYP/6-31+G(d) level of theory.

As shown in Fig. 1(a), the calculations correctly predict that the two lowest-energy conformers of IPA are those in which the COOH group is Gpy (A) and anti (B), respectively. According to the calculation, these minima are nearly isoenergetic with one another [$E(B) - E(A) = 0.022\text{ kcal/mol} = 8\text{ cm}^{-1}$]. Based on previous relaxed potential-energy scans for IPA,¹¹ the lowest-energy pathway for isomerization between these two structures involves a simple hindered rotation about the $C_\alpha\text{-C}_\beta$ bond, with a transition state in which the COOH group is eclipsed with one of the C_β hydrogens.

At the DFT $B3LYP/6-31+G(d)$ level of theory, this transition state is 2.14 kcal/mol (750 cm^{-1}) above IPA(A) minima, including zero-point energy corrections.

As explained in Paper I, in the absence of tunneling effects, the first observed transition in the PT spectrum places a firm upper bound on the energy barrier to isomerization. The last unobserved transition places a lower bound on this energy barrier if kinetic shifts are negligible, a point to which we will return shortly. We see that the calculated barrier (750 cm^{-1} for $A \rightarrow B$ and 743 cm^{-1} for $B \rightarrow A$) closely matches these experimental bounds ($800\text{--}854 \text{ cm}^{-1}$ for $A \rightarrow B$ and $644\text{--}754 \text{ cm}^{-1}$ for $B \rightarrow A$). Since movement of the entire COOH group is involved, tunneling is not likely to contribute to the dynamics appreciably.

The two lowest-energy structures computed for the IPA- H_2O complex [Fig. 1(b)] retain the gauche and anticonformation for the COOH group, with water forming a hydrogen-bonded bridge between the $\text{C}=\text{O}$ acceptor and OH donor sites. The analogous transition state separating these minima is very similar in energy (780 cm^{-1}) and structure to that in the bare molecule, consistent with the near-identical thresholds for monomer and complex observed experimentally (Table I).

4. Threshold effects

Figure 5 presents a series of SEP-PT spectra for the $A \rightarrow B$ isomerization taken with the SEP lasers at varying distances from the nozzle orifice. Since the collision rate is inversely proportional to the square of this distance, this series tests the effects of this changing collision rate on the intensities of the transitions in the spectra. Since the PT spectra measure the amount of population transferred into B from A , any changes in the intensity with collision rate reflect the competition between the energy-dependent isomerization rate and the collisional cooling rate. The collision-free SEP spectrum is given in Fig. 5(a) for comparison.

Note that the intensity of the first observed transition at 854 cm^{-1} is smaller in the $x/D=2.5$ scan [Fig. 5(b)] and gradually increases to near its relative intensity in the SEP spectrum by $x/D=4.7$. This change in x/D changes the collision rate at the point of excitation by a factor of 3.5. Note that other transitions further above threshold remain constant in size, consistent with the rate of isomerization being much greater than the cooling rate at these higher energies. In no case there is an appearance of new bands below the 854 cm^{-1} threshold, indicating that there is a negligible kinetic shift in the measured onset for isomerization in the IPA monomer. However, the observation of a change in intensity indicates that collisional cooling can compete with isomerization near threshold, and could produce larger kinetic shifts in other circumstances where the threshold isomerization rate is slower. We will take up a more quantitative discussion of these effects in the discussion section.

IV. DISCUSSION

A. Contrasting the potential-energy surfaces of IPA and TRA

Three-indole-propionic acid (IPA) differs from tryptamine (TRA), the subject of Paper I, by substitution of a

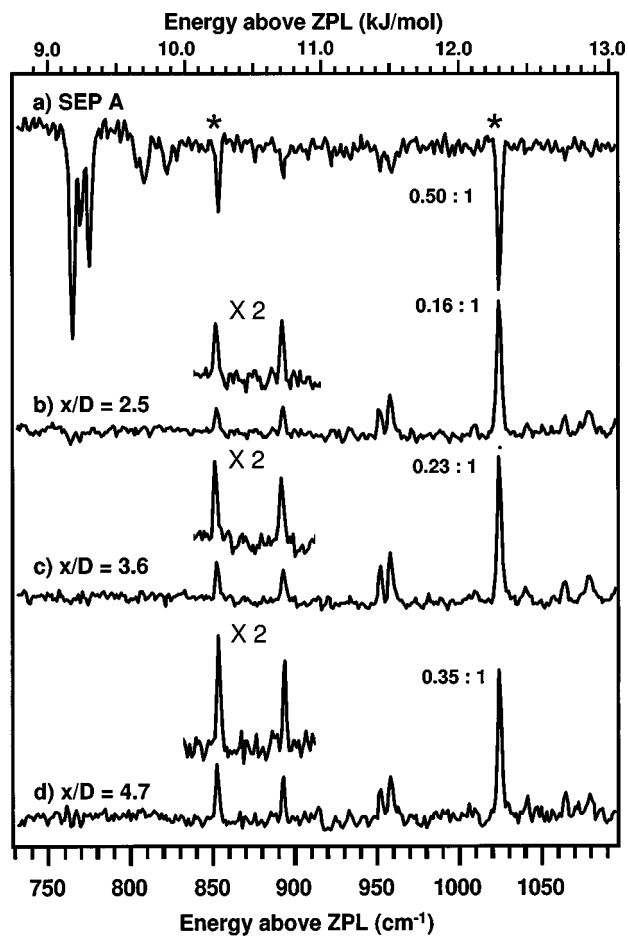


FIG. 5. (a) SEP spectrum of A. A series of SEP-PT spectra recorded with the SEP excitation at (a) $x/D=2.5$, (c) $x/D=3.6$, (d) $x/D=4.7$. The sharp onsets to population gain are shown magnified twice to highlight the increase in population gain as a function of decreasing cooling rate. The ratios of the bands marked with an asterisk exemplify the increase in gain as the cooling rate decreases. Note that in all cases, no new bands are observed to appear below the 854 cm^{-1} band.

carboxylic acid group for the amino group in the latter molecule. In an earlier publication,¹¹ we carried out a computational study of these molecules in order to understand why TRA has seven conformations with significant population under expansion cooling, while IPA has only two. By carrying out relaxed potential-energy scans along various flexible coordinates, it was established that TRA has a threefold potential for internal rotation of the NH_2 group with substantial barriers separating the minima that can trap population in the wells as cooling occurs. Furthermore, the small size of the NH_2 group, and its ability to form weak π H bonds with the indole ring, stabilize gauche minima on both the pyrrole and phenyl rings of indole. Only the Gpy(in) and Gph(in) conformers are destabilized by the repulsion between the amino lone pair and the aromatic π cloud, producing $(3 \times 3) - 2 = 7$ energetically similar minima with substantial barriers separating them.

In contrast, in IPA, the bulkier, planar COOH group prefers to have the $\text{C}=\text{O}$ group eclipsed with the $\text{C}(\alpha)\text{--C}(\beta)$ bond, only supporting shallow minima with small barriers at configurations perpendicular or antiparallel to this [Fig. 1(a)]. Furthermore, the larger size of the COOH raises the

energies of minima in the gauche position in the phenyl side of the indole ring. As a result, most of the population resides in the two lowest-energy minima in IPA, either Gpy(down) or anti(down) structures (*A* and *B*, respectively). Furthermore, population initially in the high-lying minima is efficiently funneled down into *A* or *B* under expansion cooling due to the small barriers that separate the other minima from the deep wells due to *A* or *B*.

The relaxed potential-energy scans also clarify the lowest-energy isomerization pathway connecting minima *A* and *B*. This pathway involves a simple internal rotation about the C(α)-C(β) bond that swings the COOH group from the Gpy to the antiposition. The computed barrier (750 cm^{-1}) associated with this pathway matches the experimental bounds placed on the barrier (Table I). The alternative *A*→*B* pathway would involve swinging the COOH group from the Gpy minima over the top of the ring to the Gph position and then on to the antiposition well. As already noted, the size of the COOH group creates steric hindrance to this motion, with computed barriers of more than 2000 cm^{-1} for the Gpy→Gph step.

B. The effect of water on the isomerization barrier in IPA

The spectroscopic characterization of isolated biomolecule-(H₂O)_{*n*} clusters can be used to probe the preferred binding site for the water molecule(s) and a detailed characterization of those low-energy minima. In cases where the solute has conformational flexibility, the spectroscopy can also probe the effect of water complexation on the conformational preferences of the solute. In the most extreme case, the water molecule(s) can stabilize minima in the flexible molecule that were not even stable in the absence of water. What is lacking from these spectroscopic studies is any probe of the effect of the bound water molecule(s) on the barriers to isomerization. Such data can be provided by the SEP-population transfer spectroscopy.

In the case of IPA, the carboxylic acid moiety provides an extremely stable pocket for binding of a water molecule as a hydrogen-bonded bridge between the OH donor and C=O acceptor sites. Since the IPA(*A*)→IPA(*B*) isomerization involves motion of the COOH group between the gauche and antipositions, the water molecule moves with the COOH group during the isomerization.

As we have seen, the barrier to isomerization is not changed significantly by the presence of the water molecule. This is a natural consequence of the remote position of the water molecule relative to the isomerization reaction coordinate, which involves internal rotation about the C(α)-C(β) bond. As a result, neither the isomerization reaction pathway nor the energy barrier to isomerization are changed significantly by the presence of the water molecule. We surmise on this basis that the intramolecular barrier in IPA is not sensitively dependent on the electronic character of the COOH group, which is perturbed only modestly by the presence of the water molecule.

The present data on the IPA-H₂O complex demonstrate the feasibility of studying the barriers to isomerization in

solute-solvent complexes. The mode of binding in IPA-H₂O produces little effect on the barrier to isomerization, but the example it provides also points the way to circumstances where the effect of water on the barriers to isomerization could be much more dramatic. For instance, if the water molecule were to form a H-bonded bridge between two flexible sites, then isomerization that involves these flexible sites could require the breaking of a H bond with water, substantially raising the energy barrier to doing so. Alternatively, depending on its point of attachment, the water molecule could raise the energies of certain minima on the surface, and hence effectively remove their participation in isomerization pathways available to the solute. Finally, the complexation of a solvent molecule opens up entirely new types of isomerization in which the solvent molecule moves from one site to another on the solute. This intriguing solvent rearrangement reaction can occur even in molecules without any internal flexibility. We recently have studied a first example of such a reaction in the *trans*-formanilide-H₂O complex, where SEP excitation initiates isomerization of the water molecule between two H-bonding sites on the molecule (the amide NH and C=O sites).¹²

C. The competition between isomerization and cooling

The spectra in Fig. 5 have shown clear evidence for threshold effects, in which the intensity of transitions in the SEP-PT spectra were reduced in intensity under fast-cooling conditions, indicating a competition between isomerization and vibrational cooling. In this section, we discuss the competition between isomerization and cooling and the implications of this competition on the observed thresholds.

Collisions are an integral part of the experimental protocol used here to study conformational isomerization. If both SEP excitation and detection steps were performed in the collision-free region of the expansion, SEP excitation would achieve conformation selective excitation, but conformation selective detection of the products would not be possible due to the broad absorptions of the vibrationally excited species created by the SEP process. By moving the SEP excitation into the collision-dominated region early in the expansion, the products can be recooled to their zero-point levels where they can be selectively detected without interference from one another.

As a result, isomerization necessarily occurs in competition with collisional cooling. Because the SEP process relies on adequate Franck-Condon (FC) factors to drive the population back to the ground state, only discrete internal energies can be placed into the molecule. These will bracket the true energy threshold with a grid only as fine grained as the SEP spectrum allows. If isomerization is fast compared to collisions even at threshold, then the observed onset of population transfer faithfully reflects SEP excitation overcoming that barrier. On the other hand, if isomerization was slow compared to the collisional cooling rate at threshold, then a kinetic shift would be introduced in which transitions that are above the barrier would be missed by virtue of the fast cooling.

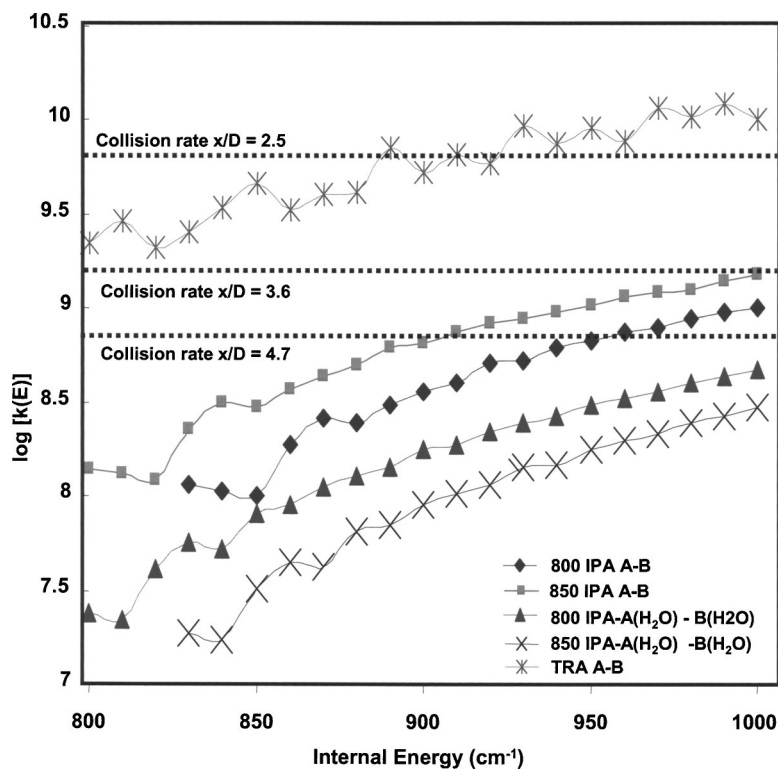


FIG. 6. The plot of $\log [k(E)]$ vs internal energy in wave numbers (cm^{-1}). The collision rate for $x/D=2.5, 3.6, 4.7$ conditions are plotted as dashed lines. The rate constant of isomerization for $A \rightarrow B$ is plotted as a diamond (\diamond) and a square (\square) for the energy threshold at 800 and 850 cm^{-1} , respectively. Likewise, the rate constant of isomerization for $A\text{-H}_2\text{O} \rightarrow B\text{-H}_2\text{O}$ is plotted for 800 cm^{-1} (Δ) and 850 cm^{-1} (\times). The rate constant for tryptamine (X) is plotted as a point of comparison (see text for discussion).

In order to understand the effects of this competition, it is helpful to first think through the process in the absence of collisions. The ground-state vibrational levels that carry the oscillator strength in the dump step are determined by the Franck–Condon (FC) factors between $S_1(0^0)$ and S_0 (Ref. 13). Large FC factors from $S_1(0^0)$ occur to vibrational levels involving normal coordinates that map along the geometry changes that accompany the electronic transition. Since the $S_0\text{-}S_1$ transition is a $\pi\text{-}\pi^*$ transition involving the indole ring, these vibrations are primarily localized vibrations of the indole ring. These zeroth-order states are anharmonically mixed with background levels at that energy. Many of the lowest-frequency vibrations of the molecule involve the flexible propionic acid side chain, and the density of states will be dominated by states with excitation in these torsional modes. Since isomerization involves some of these same torsions, intramolecular vibrational energy redistribution (IVR) into these modes must occur prior to isomerization. A harmonic density of states calculation of conformer A of IPA indicates that there are about 200 states/ cm^{-1} at an energy of $E^*=800 \text{ cm}^{-1}$. If IVR is complete within well A on a time scale faster than isomerization, then Rice–Ramsperger–Kassel–Markus (RRKM) theory predicts a threshold isomerization rate for $A \rightarrow B$ of

$$\begin{aligned} k(E^*) &= \frac{W(E^\ddagger)}{h\rho(E^*)} \\ &= 1/h \rho(E^*) \text{ at threshold} \\ &= 1.1 \times 10^8 \text{ s}^{-1}. \end{aligned}$$

Under such conditions, isomerization at threshold will be complete in IPA on the 10-ns timescale. Figure 6 shows the RRKM estimated rates for the $A \rightarrow B$ isomerization in both IPA monomer and IPA- H_2O complex. These are plotted as a

function of internal energy for thresholds of 800 and 850 cm^{-1} , the lower and upper bounds established experimentally for the isomerization in both cases.

For comparison, the analogous $A \rightarrow B$ isomerization rate in TRA is also plotted in Fig. 6 for the same threshold values. Clearly, the substitution of a light NH_2 group for COOH has decreased the density of states at a given energy and increased the calculated isomerization rate for TRA by about a factor of 20 relative to IPA. This is consistent with the lack of any threshold effects in our study of TRA in Paper I.¹

The effect of collisions will depend on the time scale of the collisions and their effectiveness in removing energy from the excited molecule. One would anticipate that collisions will accelerate IVR, destroying the coherence of the initially prepared state, and promoting the redistribution of energy into the torsional modes. Equally important, the collisions will remove internal energy and quench isomerization once the energy is brought below the barrier(s) to isomerization.

Using an estimated IPA-He cross section (σ_{coll}) of 200 \AA^2 and a backing pressure of 8-bar helium, we can estimate¹⁴ the total number of IPA-He collisions in the supersonic expansion as the IPA molecules traverse the distance between the SEP excitation ($x/D=2.5\text{--}4.7$) and the LIF detection ($x/D=6$). More importantly, the collision rate at the point of excitation can be compared with the isomerization rate. The highest collision rate occurs at $x/D=2.5$, where IPA-He collisions occur on the 250-ps timescale (Fig. 6). An extensive literature on vibrational cooling^{13,15–17} indicates that, once the density of states has reached a quasicontinuum, the fractional energy lost per collision is approximately constant; that is, $\Delta E/E=\lambda$, where λ =a constant. Based on recent studies of vibrational relaxation in N-acetyl tryptophan methyl amide (NATMA) and related molecules,

we estimated that $\lambda \sim 0.003$.^{18–20} If IPA has a similar λ value, each collision with helium would remove about 2.5 cm^{-1} per collision at 800-cm^{-1} internal energy. With this efficiency per collision, 50 cm^{-1} of internal energy (the difference between experimental lower and upper bounds) will be taken away in 20 collisions. At $x/D=2.5/3.6/4.7$, 20 collisions occur in 5/14/30 ns. This time scale is similar to that for isomerization ($\tau_{\text{isom}} \sim 7 \text{ ns}$), consistent with the observed competition between vibrational cooling and isomerization in the reduced intensity of the first observed band (850 cm^{-1}) at high collision rates.

We did not carry out a systematic study of threshold effects in IPA-H₂O. Experimentally, the first observed band appears with its full SEP intensity at 830 cm^{-1} at $x/D=2.5$, while the last unobserved band is only 30 cm^{-1} below this [Fig. 4(b)], suggesting that the isomerization rate at threshold is as large in the complex as in the monomer. However, the analogous calculations on IPA-H₂O predict RRKM isomerization rates that are slower than those in the monomer by about a factor of 5 (Fig. 6) due to the higher density of states that accompanies the addition of six low-frequency intermolecular modes in forming the complex. With a computed isomerization lifetime at threshold of about 40 ns, collisional cooling could effectively compete with isomerization near threshold. There is a partial compensation in the faster rise in rate with external energy in IPA-H₂O, due to this same increase in low-frequency modes in the transition state, but the RRKM predictions for the isomerization rate in IPA-H₂O remain below those in IPA monomer in the threshold region (Fig. 6). If isomerization near threshold is truly as fast in IPA-H₂O as in the IPA monomer, it could indicate that IVR within the modes of the IPA monomer (which leads to isomerization) occurs on a time scale fast compared to IVR to the intermolecular modes. Further experimental and theoretical studies of the effect of solvent binding on the kinetics of isomerization are clearly warranted.

V. CONCLUSION

In the present study, we have directly probed the barriers to isomerization and the relative energies of the two lowest-energy minima in both the IPA monomer and its associated single water complex. The measured upper and lower bounds bracket a barrier height for the isomerization that closely matches the computed lowest-energy barrier for the process. The comparison with theory establishes that the isomerization pathway traverses this barrier (swinging the COOH group around the outside of the indole ring between the Gpy and antipositions) rather than taking the alternative route over the top of the indole ring Gpy→Gph→anti, which has a barrier over twice as large.

Binding a single water molecule to IPA in the COOH pocket has little effect on the observed thresholds to isomerization, with upper and lower bounds nearly identical to those in the monomer. This is consistent with the computed Gpy→antibarrier, which is hardly changed by this complexation. The lack of any kinetic shift in the measurement of the threshold for the IPA-H₂O complex is at odds with a simple harmonic-based RRKM calculation of the isomerization rate relative to the anticipated vibrational cooling rate. However, the magnitude of the population transferred depends on a competition between isomerization and cooling, neither of whose absolute rates are known accurately, pointing to the need for future work.

ACKNOWLEDGMENTS

We thank the National Science Foundation for their support of this work under Grant No. (CHE-0242818). One of the authors (J.R.C.) thanks the Purdue Research Foundation for a Graduate Student Assistantship.

- ¹J. R. Clarkson, B. C. Dian, L. Moriggi, A. DeFusco, V. McCarthy, K. D. Jordan, and T. S. Zwier, *J. Chem. Phys.* **122**, xxx (2005), preceding paper.
- ²B. C. Dian, J. R. Clarkson, and T. S. Zwier, *Science* **303**, 1169 (2004).
- ³P. M. Felker, *J. Chem. Phys.* **96**, 7844 (1992).
- ⁴J. R. Carney, B. C. Dian, G. M. Florio, and T. S. Zwier, *J. Am. Chem. Soc.* **123**, 5596 (2001).
- ⁵L. L. Connell, *Structural Studies of Hydrogen-bonded Clusters using Rotational Coherence Spectroscopy*, Chemistry Department (University of California at Los Angeles, LA, 1991).
- ⁶M. J. Frisch, *et al.*, Gaussian03, in Revision B.01., Gaussian Inc., Pittsburgh, PA, 1995–2004.
- ⁷A. D. Becke, *Phys. Rev. A* **38**, 3098 (1988).
- ⁸C. Lee, W. Yang, and R. G. Parr, *Phys. Rev. B* **37**, 785 (1988).
- ⁹M. J. Frisch, J. A. Pople, and J. S. Binkley, *J. Chem. Phys.* **80**, 3265 (1984).
- ¹⁰See EPAPS Document No. E-JCPSA6-122-017523 for the complete results from the calculations including optimized geometric parameters and selected associated harmonic frequencies. This document can be reached via a direct link in the online article's HTML reference section or via the EPAPS homepage (<http://www.aip.org/pubservs/epaps.html>).
- ¹¹J. R. Carney and T. S. Zwier, *Chem. Phys. Lett.* **341**, 77 (2001).
- ¹²J. R. Clarkson, E. Baquero, V. A. Shubert, E. M. Myshakin, K. D. Jordan, and T. S. Zwier, *Science* **307**, 1443 (2005).
- ¹³J. R. Barker, *J. Phys. Chem.* **88**, 11 (1984).
- ¹⁴D. M. Lubman, C. T. Rettner, and R. N. Zare, *J. Phys. Chem.* **86**, 1129 (1982).
- ¹⁵J. Troe, *Pure Appl. Chem.* **69**, 841 (1997).
- ¹⁶M. Damm, F. Deckert, H. Hippler, and J. Troe, *J. Phys. Chem.* **95**, 2005 (1991).
- ¹⁷G. W. Flynn, C. S. Parmenter, and A. M. Wodtke, *J. Phys. Chem.* **100**, 12817 (1996).
- ¹⁸D. Evans, D. Wales, B. C. Dian, and T. S. Zwier, *J. Chem. Phys.* **120**, 148 (2004).
- ¹⁹B. C. Dian, A. Longarte, P. R. Winter, and T. S. Zwier, *J. Chem. Phys.* **120**, 133 (2004).
- ²⁰B. C. Dian, G. M. Florio, J. R. Clarkson, A. Longarte, and T. S. Zwier, *J. Chem. Phys.* **120**, 9033 (2004).